OBJECT VOLUMETRIC ESTIMATION BASED ON GENERIC FITTED PRIMITIVES FOR SERVICE ROBOTICS

Tiberiu T. Cociaș, Sorin M. Grigorescu and Florin Moldoveanu

Departament of Automation, Transilvania University of Brașov, Brașov, Romania

{tiberiu.cocias, s.grigorescu, moldof}@unitbv.ro

Keywords: Robot vision, 3D object reconstruction, Surface approximation, Primitive fitting, Service robotics.

Abstract: This paper present an approach for object surface estimation from a single perspective using a stereo camera configuration. The goal of the method is to capture the particularity of an object of interest by fitting a generic primitive who best models the recognized shape. The shape modeling process is performed on 3D *Regions of Interest* (ROI) obtained by classifying the objects present in disparity maps. The principle uses a number of *control points*, calculated from the primitive *Point Distribution Model* (PDM). These control points drive the modeling behavior in the disparity point cloud data based on the principle of active contours, or snakes. Finally a compact 3D object mesh can be generated using Delaunay triangulation. The obtained PDM models are intended to be used for the purpose of precise object manipulation in service robotics applications.

1 INTRODUCTION

Nowadays most service robotics applications use depth perception for the purpose of environment understanding. In order to precisely locate, grasp and manipulate an object, a robot has to estimate as good as possible the pose and the structure of that object of interest. For this reason different visual acquisition devices, such as stereo cameras, range finder or structured light sensors, are used (Trucco and Verri, 1998).

For online manipulation, together with the pose of the object, it is needed to determine the 3D particularities of the viewed structure in order to estimate its shape (Hartley and Zisserman, 2004).

There are several types of methods that focus on the 3D reconstruction of objects using multiple perspectives. Such methods try to reconstruct the convex hull of the object (Matsuyama et al., 2004), or to recover its photo-hull (Kutulakos and Seitz, 2000). Other algorithms explore the minimization of the object's surface integral with a certain cost function over the surface shape (Lhuillier and Quan, 2005).

On the other hand, the reconstruction can be addressed also from a single view. This technique is usually efficient when applied to regular surface objects. An early approach for this challenge was investigated for piecewise planar reconstructions of paintings and photographs (Horry et al., 1997). Subsequent improvements of the technique (Criminisi et al., 2000), (Sturm and Maybank, 1999) increased the geometric precision especially for scenes with multiple vanishing planes.

In terms of reconstruction resolution and accuracy, range images (e.g. from laser scanners) provide one of the best surface estimations from all techniques. However, it has speed deficiency, sensor dimension and power consumption (Kim et al., 2009).

The main challenge encountered during 3D reconstruction is the automatic computation of the 3D transformations that align the range data. Thus, the registration of different perspective point clouds into one common coordinate system represents one of the most researched topics in the vision community (Kim, 2009), (Stamos et al., 2008).

The rest of the paper is organized as follows. In Section 2 a brief description of the image processing chain is provided. The main contribution of the paper, that is the 3D shape modeling approach, is given in Section 3. Finally, before conclusions, performance evaluation results are presented in Section 4.

2 MACHINE VISION APARATUS

The block diagram of the proposed scene perception system can be seen in figure 1.

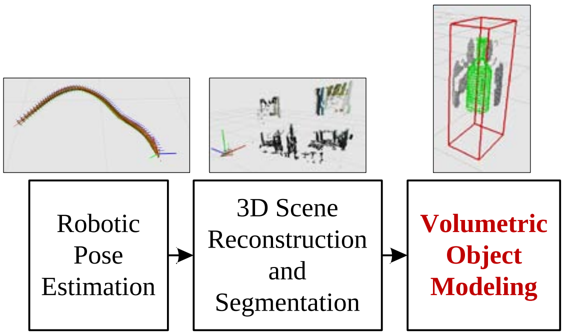

Figure 1: Block diagram of the proposed scene perception system.

The reference coordinates of the obtained visual information is related to the on-line determined *position and orientation* (pose) of a robot, that is, of a robot's stereo camera system (Grigorescu et al., 2011). Once a certain pose is determined, the imaged scene can be reconstructed and segmented for the purpose of environment understanding. The main objective here is to get the depth, or disparity, map which describes the 3D structure of an imaged scene. This information is further used by the final *object volumetric modeling* algorithm, which is actually the main focus of this paper. One of the main algorithms used in the proposed vision system is the object classification method which delivers to the volumetric modeling method the object class and the 2D object ROI. The classification procedure is based on color and depth information. A detailed description of the approach can be found in (Grigorescu et al., 2011).

3 OBJECT VOLUMETRIC MODELLING

The object volumetric modeling system is based on the active contour principle used to manipulate a set of pre-defined *Point Distribution Models* (PDM) by stretching them over a disparity point cloud describing an object in a given *Region of Interest* (ROI). In the considered process, three main challenges arise: *the sparse nature of the disparity maps, the calculation of the 3D ROI* and *the nonlinear object modeling*.

3.1 PDM Primitive

In the presented work, an *object generic primitive* is defined as a PDM model which serves as a backbone element forconstructing a particular object, or shape. The generic PDM primitive is represented by a data structure that has as background component a shape vector $\boldsymbol{X}$ which contains 3D feature points describing the model of an object class. Such example models are shown in figure 2. Additionally, the structure contains a scale factor s, a rotation matrix R and a translation matrix t that relates the PDM to a canonical reference coordinate system.

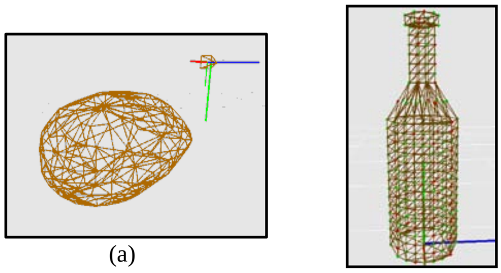

(a) (b)

Figure 2: Generic meshed PDM models. (a) Potato. (b)Bottle.

Since in the considered source of visual information, that is disparity images, only one perspective of the imaged object is available, the PDM model is actually used to compensate for the missing information. In this case we consider objects that have a symmetrical shape. Nevertheless, the proposed approach can be applied on irregular shaped entities. Depending on the complexity and regularity of the surface object, the primitive model can be defined either by a low or a high number of 3D feature points. For example, the bottle shown in figure 2 is described by 382 feature points. Since the PDM describing such an object represents a regular surface, not all these points are important for the object modeling process. The so-called *control points*, namely those points that define the shape of an object, can be automatically determined based on three main characteristics (Cootes, 1995):

1. Points marking the center of a region or sharp corners of a boundary;
2. Points marking a curvature extreme or the highest point of an object;
3. Points situated at equal distance around a boundary between two control points obeying rule one.

In the same time, control points can be determined manually under the guidance of a human (Zheng et al., 2008). This last method captures the features of an object more efficiently but suffers from subjectivity on features definition since the process is controlled by a human person. Depending on the modeled object, in our approach we used both the automatic and the manual techniques to determine control points. Using the introduced points, the computation time is increased since the number of points describing the shape of an object is usually much lower than the total number of points from the PDM. The 3D positions of the PDM points are actually directly dependent on the positions of the control points, as it will later be shown in this section. For example, from a total of 382 points describing the bottle primitive from figure 2(b), only 71 of them (marked with red dots) are considered to be control points. On the other hand,for a complex object, this number can be equal to the initial PDM features number, meaning that all points from the primitive are considered to be control points since all of them are needed to capture a specific feature. Taking into account a lower number of control points will considerably increase the computational speed of the modeling process.

3.2 Disparity Map Enhancement

As opposed to newer structured light sensors, such as the MS Kinect®, one main drawback of the considered visual information is the sparse 3D structure of disparity maps. Namely, it contains "holes" or discontinuities in areas where no stereo feature matching exists (Brown, 2003). Such discontinuities are present in low textured regions or constant color areas from the environment.

To overcome this issue we propose an enhancement method which deals with disparity maps discontinuities. Basically, the idea is to scan each point from a disparity image and determine if there is a gap between the considered point and a neighboring point situated at a certain distance, as shown in figure 3(a). Since we apply the principle on disparity maps, which are defined on the 2D domain, there are only 5 main neighboring directions from a total of 8 in which we search for discontinuities. The untreated 3 directions refer to the back of the centered point and it is assumed that are no discontinuities in that direction since the position is already searched.

The disparity map is actually a grey scale image with pixel intensities inverse-proportional to the distance between the considered 3D world point and the camera's position. Having in mind that the disparity image is represented using 8 bits, we sample it using 256 layers, each corresponding to certain intensity in the disparity domain. The enhancement process searches for discontinuities only in one layer at a time, since there is no information about the connectivity of the intensities. In this sense, the layers are stored using a 256 bins histogram. For each pixel in each layer the number of the same intensity along a direction is calculated. In order not to merge two different objects, the search area is reduced to a finite value, dynamically calculated. The search process starts from the lowest neighboring distance value, which has a two pixels length, and ends when a discontinuity is found or the maximum length is reached. The discontinuity is determined by comparing the length of the direction with the number of the same intensity pixels found along this direction. If the number of pixels found is below the length of the considered direction, the missing positions are filled with pixels with the same intensity as the ones alreadyfound.

There is a slight chance that two closely positioned objects are merged by the algorithm. In order to overcome this challenge, a variance driven image of the disparity map has been used (Turiac et al., 2010). From the variance image only object contours are extracted. In this way it can be determined if the points which take part in the fill process belong to one single region or to a neighboring region. The result of the presented method will be a compact and dense representation of the disparity image, as shown in figure 3(c). On the other hand, it is needed to connect the layers

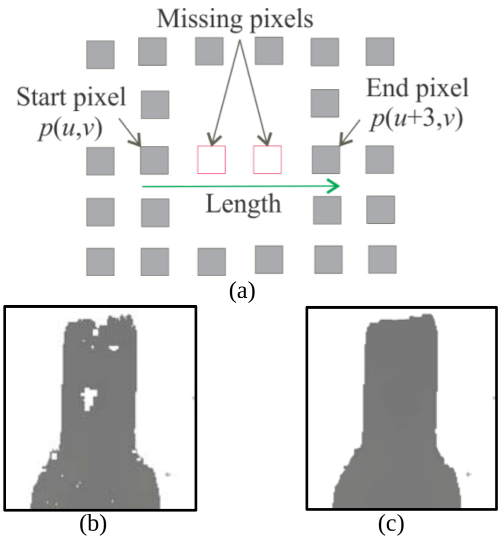

Figure 3: Disparity enhancement algorithm. (a) Missing pixels searching principle. (b)Original disparity map. (c) Enhanced disparity image.

which are very close (in terms of disparity) in the 3D model. This can be achieved by diffusing the gradient separating two neighboring intensities. In order to preserve the 3D features of the object, the diffusing process will occur only for regions with translation of intensity no grater then 5 intensities layers. In this way, the obtained layers are smoothly connected.

3.3 3D ROI Definition

The 2D segmentationand classification process provides, besides the class to which the object belongs, a ROI feature vector $[p_{L_i}, p_{R_i}]$, $i = 1,2,3,4$ defined in the stereo image pair domain. This description restricts the object search area to a quadratic region of interest. By computing the disparity between the left and right ROI points we obtain a 3D representation of the considered ROI. In this way only a planar representation (slice)in the 3D space is obtained. The volumetric property is evaluated starting with the assumption that the pixels inside the 2D ROI describe only the object. The depth is determined statistically by finding the highest density of 3D points which lie inside the planar ROI along the *Z* 3D Cartesian axis. A 3D representation of the ROI can be seen in figure 4. However, there is a possibility that the highest density of 3D points belongs to a noise entity outside the object border but still inside the ROI.

To overcome this problem, a histogram of the disparity image is calculated. Instead of searching only the top density value of the intensities in histogram, we check also the highest aperture of the histogram for the considered top density. Basically we determine the highest distribution of connected points by summing all the densities from the slices of the aperture belonging to a top value of the histogram as:

$$d = \sum_{i+a}^{i+b} \max(h(i)), \tag{1}$$

Where d represent the highest cluster of 3D points, $h(i)$ is the number of pixels for a certain bin i and a, b are the closest and farthest non zero $h(i)$relatively to the considered intensity i, respectively. The margin of the aperture is actually defining the first and last planes of the 3D ROI volume along the *Z* axis, respectively.

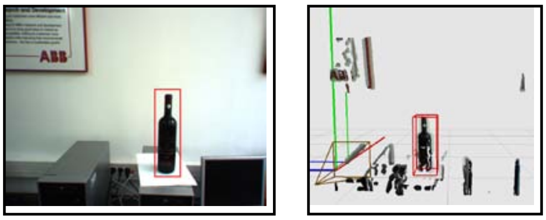

(a) (b)

Figure 4: 3D ROI computation. (a) Input image together with the calculated 2D ROI. (b) 3D ROI reprojection.

3.4 PDM Shape Alignment

The 3D alignment process deals with the calculation of the rotation and translation of the primitive shape with respect to the point cloud distribution of the disparity information inside the 3D ROI. Because each PDM, that is primitive and point cloud, is defined in its own coordinates system, a *similarity transformation*is used to align the two models. Since the ROI's PDM is related to the same coordinate system as the 3D virtual environment, we have chosen to bring the primitive's PDM into a reference 3D environment coordinate system. The reference coordinate system is given by the on-line determined pose of the stereo camera (Grigorescu et al., 2011). In this sense, the primitive is considered to be a translational shape, while the 3D ROI is marked as a static cube. The similarity transformation is described by:

$$X_{new} = sR(X_{old} - t), \tag{2}$$

where, X_{old} and X_{new} represent the 3D coordinate of a point before and after the similarity transformation, s is a scale factor, while R and t are the matrices defining the rotation and translation of a point, respectively. These coefficients represent the *Degrees of Freedom* (DoF) of a certain shape.

The scale factor is determined based on the 3D point cloud information inside the ROI. Since a disparity enhancement is considered before the 3D reprojection process, it can be presumed that inside the ROI exist one or more large densities of points which describe the object of interest. Thus, by evaluating the distribution of these densities we can compute a percentage of the size difference between the object PDM shape and the point cloud within the 3D ROI.

The translation of the moving shape is easily determined by adding the center of gravity of the points inside the 3D ROI from the center of gravity of the primitive PDM, as follows:

$$t = \frac{1}{n_p}\sum_{i=1}^{n_p} a + \frac{1}{n_p}\sum_{i=1}^{n_p} b \qquad (3)$$

where, n_p represent the number of points of the model and a and b are the two densities of points, that is of the object's shape (primitive model) and of the fixed point cloud inside the 3D ROI. The rotation matrix R is determined by evaluating the 3D distribution of the disparity point cloud information, that is, 3D slope from which the point data is aligned.

By using the proposed alignment method, a rough object volumetric estimation is obtained based on the fitting primitive principle. An example result of the similarity transformation can be seen in figure 5, where, the green silhouette represents the PDM primitive shape.

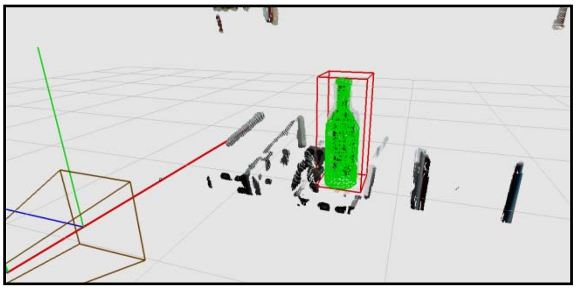

Figure 5: Primitive PDM shape alignment example.

3.5 PDM Primitive Modeling

The points which drive the modeling process are the control points described in a previous subsection. The behaviorof the other points in the PDM model is automatically derived from the movement of the control points. The modeling process is achieved by dragging after each control point the neighbors from the surrounding area. Each of the neighbor point is moved based on a physical relation describing the property of the considered object. This relation can be either linear, as in equation 4, or non-linear for more complex surfaces. For simplicity if explanations, we have considered in this work a linear relation between control and the rest of the PDM points:

$$X_{new} = X_{old}\left(1 + \frac{d_{curr}}{d_{\max}}\right), \qquad (4)$$

where, X_{new} and X_{old} represent the new and old 3D coordinates of the considered neighboring points, respectively, $d_{\max}$ is the distance between the control point and the farthest neighbor within the affected area and d_{curr} represent the distance between the control point and the translated neighbor. The results of such a linear modeling are shown in figure 6, where control points are marked with red, their neighbors are labeled with blue the rest of the PDM points are green.The surrounding dragged area has the shape of a cube centered on the control point 3D coordinate and has its area defined as double the distance between the initial and the new position of the control point, as depicted in figure 5.

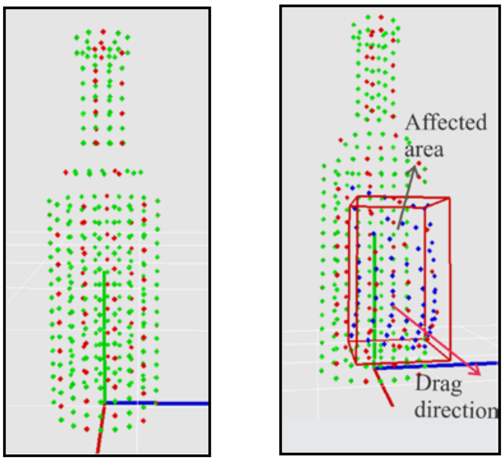

(a) (b)

Figure 6. A linear dependency between a control point and its neighbors. (a) Initial PDM shape model.(b) Point deformation along a considered direction.

The proposed approach for estimating an object's volume starts with a generic object PDM model, namely a primitive, and ends by capturing by each primitive control point the local features of the modeled object of interest. As explained, this is achieved by minimizing the distance between the control point and the PDM in a respective neighborhood. The minimization procedure is based on the *active contours* principle, better known as *snakes* (Kass et al., 1988). This approach represents a deformable contour model of the considered object.

In an image, an active contour is a curve parameterized by the minimization of and energy functional:

$$\varepsilon(c) = \varepsilon_{\text{int}}(c) + \varepsilon_{ext}(c) = \int_0^1 [E_{\text{int}}(c(s)) + E_{ext}(c(s))]ds, \tag{5}$$

where, E_{int} and E_{ext} are the internal and external energies, respectively and $c(s) = [x(s), y(s), z(s)]$ represents the curve describing the object's surface. while $s \in [0,1]$. By defining an initial contour within an image, it will move under the influence of internal forces computed based on the derivatives from the active contour an also under the influence of the external forces captured from the image.

In the presented 3D object modeling approach, the disparity image domain is equivalent to the 3D representation of the scene. For this reason the same energy minimization principle has been used to model the shape of an object. Instead of using an initial active contour, as in the original method, we propose the use of a 3D generic primitive PDM model. The movement of the contour surface is thus described by the direction of the lowest functional energy, that specific region actually corresponding to aprobable contour in the image (Mark et al., 2002). In the considered 3D case being the highest density of points from the 3D scene.

The idea of using forces to move the primitive points is that the primitive PDM must be attracted and fitted on the border of the object. The internal forces, which refer exclusively to the primitive PDM, are responsible for supervising the shape smoothness and continuity. As described in the equation 6, the continuity property is controlled by the first derivate while smoothens is define by the second derivate of the surface.

$$E_{\text{int}} = E_{cont} + E_{curv} = \frac{1}{2}(\alpha(s)\left|v^{'}(s)\right|^2 + \beta(s)\left|v^{''}(s)\right|^2), \tag{6}$$

where, E_{cont} is the energy responsible for the continuity of the surface and E_{curve} deals with the bending property of the hull of the object. α and β are two parameters which influence the E_{cont} and E_{curve} forces, while $v(s) = [x(s), y(s), z(s)]$ represent the coordinates of a point from the shape vector $\boldsymbol{X}$. In the discreet domain the two energies can be rewritten as:

$$E_{cont} = (x_i - x_{i-1})^2 + (y_i - y_{i-1})^2 + (z_i - z_{i-1})^2 \tag{7}$$

$$\begin{aligned} E_{curv} = {} & (x_{i-1} - 2x_i + x_{i+1})^2 + (y_{i-1} - 2y_i + y_{i+1})^2 \\ & + (z_{i-1} - 2z_i + z_{i+1})^2, \end{aligned} \tag{8}$$

where, $x_i, y_i, z_i \in \mathbf{X}$, $i = 1...n_p$ and n_p is the number of points in the shape PDM vector. In the original formulation of the principle, each point from the shape can be moved in one of the eight possible 2D directions. In current3D approach, because of the third dimension, a number of 24 directions are taken into account.

The correct moving direction is mainly influenced by the external energy E_{ext} which evaluates for each direction the highest density of 3D points. Because this density can be spatially very close, a weight factor for the external energy is introduced. Thus, if these candidate positions have an appropriate number of points, the weight factor will be considered zero.

Since we have only one perspective of the object, there are large object areas with no 3D point cloud description needed to drive the contour energies. The un-imaged back side of an object represents such an example. In the proposed approach, the missing information is filled by the generic data introduced by the PDM primitive model.

4 EXPERIMENTAL RESULTS

For evaluation purposes, a Point Grey Bumblebee® stereo camera system mounted on an autonomous platform equipped with a robotic manipulator was used. The objects used during tests were placed at random location on flat surfaces present. The exact location of an object is unknown. We tested the algorithm on two different types of objects, namely bottles and potatoes having different irregular shapes. The bottles object class represents a large number of geometrical regular shapes frequently encountered in domestic settings. The potato is used to test the algorithm against complex irregular surfaces.

The *Ground Truth* (GT) data against which the proposed method has been tested is composed of a number of manual measurements conducted on the objects: width, height, thickness, translation and rotation. The translation and rotation was measure with respect to a fixed reference coordinate system represented by an ARToolKit® marker.

Table 1: Performance evaluation results for the proposed volumetric modelling system.

Shape		Width[m]	Height[m]	Thickness[m]	Φ[deg]	θ[deg]	φ[deg]	x[m]	y[m]	z[m]
Bottle	GT	0.085	0.35	0.08	0	1.3	5.7	0.1	0.05	0.850
	Online	0.086	0.3491	0.0749	1.121	2.12	5.27	0.088	0.061	0.869
Potato	GT	0.087	0.059	0.06	0	2.5	1.5	0.1	0.05	0.850
	Online	0.0855	0.0637	0.0651	2.08	1.67	-0.38	0.09	-0.055	0.873

Because of its regular shape, the volumetric estimation of bottles had the lowest modeling error, as can be seen from Table. 1. The modeled primitive captured efficiently the particularity of the surfaces, thus resulting in a precise surface estimation. On the other hand, due to their irregular shape, a higher estimation error has been determined for the considered potatoes. An example of obtained test results can be seen in Table 1, were Φ, θ and φ are Euler angles and *x*, *y*, and *z* are positions along the three Cartesian axes, respectively.

5 CONCLUSIONS

In this paper, an object volumetric modeling algorithm for objects of interest encountered in real world service robotics environments has been proposed. The goal of the approach is to determine as precisely as possible the 3D particular surface structure of different objects. The calculated 3D model can be further used for the purpose of visually guided object grasping. As future work the authors consider the time computation enhancement of the proposed procedure through parallel computational devices (e.g. Graphic Processors), as well as the application of the method to other computer vision areas, such as 3D medical imaging.

ACKNOWLEDGEMENTS

This paper is supported by the Sectoral Operational Program Human Resources Development (SOP HRD), financed from the European Social Fund and by the Romanian Government under the projects POSDRU/107/1.5/S/ 76945 and POSDRU/89/1.5/S/59323.

REFERENCES

Brown, M., Burschka, D., Hager, G. 2003. Advances in Computational Stereo, *IEEE Transaction on Pattern Recognition and Machine Intelligence*, 25(8):993–1008.

Cootes, T., Taylor, C., Cooper, D., Graham, J. 1995. Active Shape Models-Their Training and Application, *Comp. Vision and Image Understanding*, 61(1):38-59.

Criminisi, A., Reid, I., Zisserman, A. 2000. Single View Metrology, *International Journal on Computer Vision*, 40(2):123–148,

Grigorescu, S., Cocias, T., Macesanu, G., Puiu, D., Moldoveanu, F. 2011, Robust Camera Pose and Scene Structure Analysis for Service Robotics, *Robotics and Autonomous Systems*, 59(11):899-909.

Hartley,R., Zisserman, A. 2004. *Multiple View Geometryin Computer Vision*, Cambridge University Press.

Horry, Y.,Anjyo, K., Arai, K. 1997. Tour into the Picture: Using a Spidery Mesh Interface to Make Animation from a Single Image, *Proc. ACM SIGGRAPH.*

Kass, M., Witkin, A., Terzopoulos, D. 1998. Snakes: Active Contour Models, *International Journal of Computer Vision*, 1(4):321-331.

Kim,T., Seo,Y., Lee,S., Yang,Z., Chang,M. 2009 Simultaneous Registration of Multiple Views with Markers,*Computer-Aided Desig*n, 41(4):231–239.

Kutulakos, K., Seitz, S. 2000. A Theory of Shape by Space Carving, *International Journal of Computer Vision*, 38(3):199–218.

Lhuillier, M., Quan, L. 2005. A Quasi-Dense Approach to Surface Reconstruction from Uncalibrated Images, *IEEE TPAMI*, 27(3):418–433.

Matsuyama, T., Wu, X., Takai, T., Wada, T. 2004. Real-Time Dynamic 3-D Object Shape Reconstruction and High-Fidelity Texture Mapping for 3-D Video, *In IEEE Transactions on Circuits and Systems for Video Technology*, 14(3), 357–369.

Stamos, I., Liu, L., Chao, C., Wolberg, G., Yu, G., Zokai, S. 2008. Integrating Automated Range Registration with Multi-view Geometry for the Photorealistic Modeling of Large-Scale Scenes. *International Journal of Computer Vision*, Springer, 78(2/3):237–260.

Sturm, P., Maybank, S. 1999. A Method for Interactive 3D Reconstruction of Piecewise Planar Objects from Single Images, *In BMVC*.

Trucco, E., Verri, A. 1998.*Introductory Techniques for 3-D Computer Vision*, Prentice Hall PTR.

Turiac, M., Ivanovici, M.,Radulescu, T. 2010.Variance-driven Active Contours, *International Conference on Image Processing, Computer Vision, and Pattern Recognition*.

Zheng, Y., Barbu, A., Georgescu, B., Scheuering, M., and Comaniciu, D. 2008. Four-Chamber Heart Modeling and Automatic Segmentation for 3D Cardiac CT Volumes Using Marginal Space Learning and Steerable Features,*IEEE Transaction on Medical Imaging*, 27(11):1668–1681.